International Journal of Engineering & Technology, 7 (4.10) (2018) 28-33

International Journal of Engineering & Technology

Website: www.sciencepubco.com/index.php/IJET

Research paper



Band Selection Using SIFT in Hyperspectral Images

M.R.Vimala Devi[1]*, S.Kalaivani[2]

[1,2]School of Electronics Engineering,VIT University,Vellore,India.
**Corresponding author E-mail: madhumrvd@gmail.com*

Abstract

In this paper an approach for dimension reduction of the hyperspectral image using scale invariant feature transform (SIFT) is introduced. Due to high dimensionality of hyperspectral cubes, it is a very difficult task to select few informative bands from original hyperspectral remote sensing images. Band with maximum amount of non-redundant information are chosen using the dissimilarity matrix obtained from scale invariant feature transformed image. The performance of the dimension reduction technique is analyzed by implementing a post-processing technique named spectral un-mixing. Spectral unmixing is the process of extracting end members and generating their abundance maps. End members are extracted with these selected informative bands using N-FINDR and abundance maps are generated using fully constrained least square estimation. The simulation software used for implementation of algorithms is MATLAB. Qualitatively and quantitatively the proposed feature based approach has been analyzed with application to spectral unmixing by comparing with two well-known existing dimension reduction techniques namely principal Component Analysis and Linear Discriminant Analysis. Hyperspectral images finds application in astronomy, agriculture, geosciences and surveillance.

Keywords: *Band selection; Hyperspectral Image; Principal component analysis; Scale invariant feature transform; Spectral unmixing.*

1. Introduction

In recent years, spectral processing plays a major role in the field of image processing. Spectral information greatly facilitates auto processing compared to spatial processing. Generally remote sensing obtains the spectral radiation of a pixel based on radiation reflected from all the objects in the ground instantaneous field of view [1]. Remote sensing images are classified as multispectral, hyperspectral and ultraspectral images on the basis of measurement type and number of bands [2]. Hyperspectral sensors in the visible portion of the electromagnetic spectrum collect hundreds of narrow and continuously spaced spectral bands of data known as hyperspectral cubes or hyperspectral images [9]. Hyperspectral cubes used for analysis is of three dimension represented by f(x,y,λ) where λ is the wavelength of the band. Hyperspectral images are spatially registered and rich in spectral information in which each pixel contains detailed information about the spectrum of incoming light. The spectrum of each pixel in the image represents a unique spectral signature of a material which helps in finding sub-pixel objects, identifying materials or detecting processes which are spectrally similar [20]. A sensor of NASA's airborne and spaces borne with its hyperspectral instrument are used to obtain hyperspectral images or cubes.

Let us consider $Z \triangleq [Z_1, Z_2.., Z_N]^T \in R^{NXP}$ be the lexicographically indexed HSI composed of P pixels and N bands, where $z_n \triangleq [z_{n,1}, z_{n,2}.., z_{n,N}]^T$ is the image observed in the n^{th} band corresponding to a wavelength λn. The pixel value Z_{ij} is the reflectance of the j^{th} image pixel to the i^{th} frequency band [4]. The reflectance value measured Z_{ij} is to be decomposed into its basic elements or end members and this process is known as spectral unmixing. With reference to hyperspectral image Z,the spectral unmixing is the problem of finding the end member matrix $V \in R^{NXK}$ and the abundance matrix $A \in R^{KXP}$.The factor K denotes the number of elements or end members whose value is less than min(N,P) [18].The hyperspectral image Z can be denoted as $Z \approx VA$ in terms of end member 'V' and abundance matrix 'A'. The main problem with this hyperspectral data is its huge dimension [2]. The three main issues related to high dimension of hyperspectral data are high storage and transmission problem, redundancy and high processing time. Dimension reduction is the only pre-processing technique that can be used to overcome these issues and also it helps to achieve accurate results in subsequent post processing techniques like spectral unmixing and classification. In general there are two ways of reducing the dimension of hyperspectral images namely transform based and band selection based techniques. Each of the type has its own advantages and disadvantages. Principal Component Analysis (PCA) is an example of transform based and any supervised or unsupervised method is an example for band selection based technique. Various techniques for dimension reduction are PCA, Discriminant Analysis, and Minimum Noise Fraction (MNF) etc [5].

In this paper, we propose a feature extraction based dimension reduction of hyperspectral images. The proposed method reduces the dimension by eliminating bands which are highly correlated and maximum statistical dependence to each other. To highlight the performance of the proposed dimension reduction technique, the post processing method namely Spectral Unmixing is implemented in MATLAB. Spectral unmixing is the process of decomposing the pixel into its end members and abundance maps [10].

The paper sub sections are as follows, problem is formulated in section 2,the hyperspectral data used is detailed in section 3,band selection using SIFT is explained in section 4 , end member extraction algorithm is discussed in section 5 and 5.1, abundance map algorithm is discussed in section 5.2. The proposed work is detailed in the section 6. Implementation of the algorithms is explained in section 7. Summary and extension of the work is given n section 8.

Copyright © 2018 Authors. This is an open access article distributed under the Creative Commons Attribution License, which permits unrestricted use, distribution, and reproduction in any medium, provided the original work is properly cited.

2. Problem Formulation

Hyperspectral cubes or hyperspectral images contain hundreds of bands compared to other remote sensing images [16]. If, we denote 'Z' as an image with R rows and C columns then hyperspectral image can be denoted as Z_{RxCxN} where 'N' represents the number of bands. The huge number of bands with more redundant information must be reduced for any application like, unmixing, classification and change detection. In this paper, feature based band selection followed by unmixing application has been implemented [7]. Modeling hyperspectral unmixing is a difficult problem since it depends on how the pixels are mixed either in a linear or non-linear fashion [20]. Mathematically, linear mixture model is formulated as

$$y(n) = \sum a_i S_i(n) + v(n) \quad (1)$$

Where *i* represents the number of end members, a_i denotes abundance vector , $S_i(n)$ denotes spectral signature vector and $v(n)$ denotes noise[11].

The steps involved in extracting the spectral signatures and abundance maps to highlight the dimension reduction technique are as shown in Fig.1. In the original hyperspectral image, as an initial step the signal to noise ratio is calculated for each band and band with minimum signal to noise ratio is removed [3] .

Then the number of end members 'p' or spectral signatures are estimated using virtual dimensionality algorithm [2], followed by reducing hundreds of bands to 'p' number of bands. This 'p' set of bands are processed using end member extraction technique to obtain spectral signatures and their abundance maps are generated using FCLS [16].

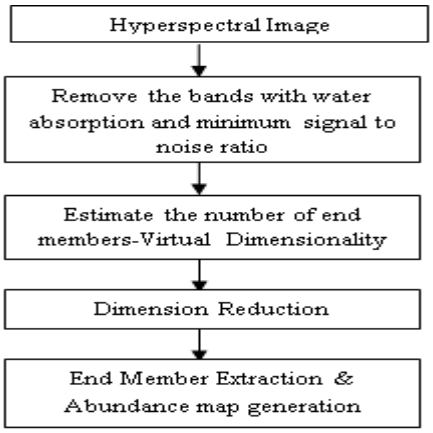


Fig.1: Flow Chart of Hyperspectral Unmixing.

3. Hyperspectral Data

Jasper Ridge, AVIRIS hyperspectral data of size 512X614 pixels with 224 bands ranging from 380nm to 2500nm is taken as input data. Its spectral resolution is 9.46nm.To reduce the computational complexity, resized image of 100 X 100 is taken as input data [20].

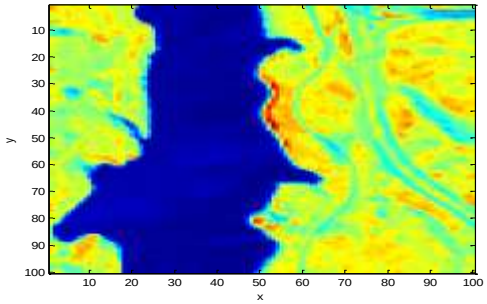


Fig.2: Jasper Ridge Reflectance image at band 90

Samson image,AVIRIS hyperspectral data of size 95X95 pixels with 156 bands ranging from 380nm to 2500nm is taken as another input data. Its spectral resolution is 9.46nm. To reduce the computational complexity, resized image of 100 X 100 is taken as input data [20].

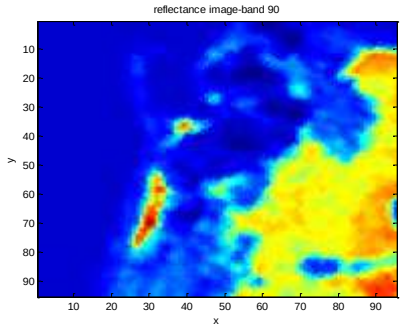


Fig.3: Samson Reflectance image at band 90

4. Scale Invariant Feature Transform

Feature extraction algorithm are based on extracting the features which are informative, non-redundant and their by resulting in a reduced dimension image with respect to its original. The features selected contains more relevant information from the input image so that the reduced set of images helps to perform the desired task as efficiently as with original large dimension image. Few of the feature extraction algorithm are FAST (Features from Accelerated Segment Test),SURF(Speeded UP Robust Features) SIFT (Scale Invariant Feature Transform) and PCA-SIFT(Principal Component - SIFT).In this paper, we have used SIFT as feature transform technique due to its stability, robust and invariant to translation ,scaling ,rotation, blur and illumination changes [6].

The highly distinctive invariant features are extracted from images using scale invariant image feature transform [13] .SIFT algorithm is implemented in four steps namely scale space extrema detection, location of key points, orientation assignment and key point descriptor. The main idea of this algorithm is, it first extracts key points for all band images in hyperspectral data and bands are matched using Euclidean distance. Based on the matching score, bands are selected for further processing with the help of dissimilarity matrix [19].

The detailed steps to extract SIFT descriptor are as shown in Fig. 4.

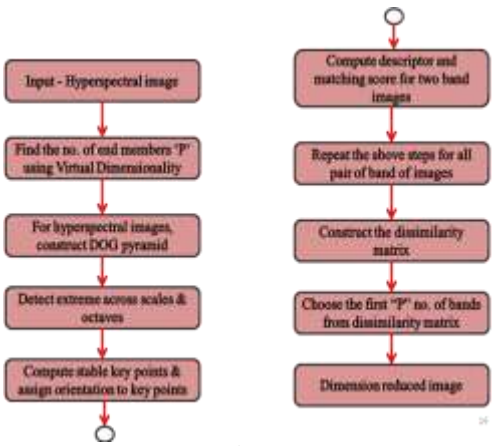


Fig.4: Flowchart of SIFT Algorithm

Hyperspectral image is taken as an input and the number of end members are calculated using virtual dimensionality algorithm .Then the scale space of an image $s(l, m, \sigma)$ is obtained by convolving the input image $z(l, m)$ with Gaussian function $g(l, m, \sigma)$.

$$s(l,m,\sigma) = g(l,m,\sigma) * z(l,m) \quad (2)$$

where

$$g(l,m,\sigma) = \frac{1}{2\pi\sigma^2} e^{\frac{-(l^2+m^2)}{2\sigma^2}}$$

To detect key point locations better, the Gaussian function is replaced with difference of Gaussian function $DOG(l,m,\sigma)$.

$$DOG(l,m,\sigma) = [g(l,m,k\sigma) - g(l,m,\sigma)] * z(l,m) \quad (3)$$

$$DOG(l,m,\sigma) = [s(l,m,k\sigma) - s(l,m,\sigma)] \quad (4)$$

After obtaining $DOG(l,m,\sigma)$, local maxima and minima for each sample point is detected by comparing it with its neighbours in the current image, one scale above and below. If a particular location point is not matching with its neighbors, then that point is selected [6].

To make the location computation more accurate, sub pixel localization is used .For each and every location, magnitude and orientation is obtained using equation (5) - (6) .

$$mag(l,m) = \sqrt{(s(l+1,m)-s(l-1,m))^2 + (s(l,m+1)-s(l,m-1))^2} \quad (5)$$

$$\theta(l,m) = \tan^{-1}\left(\frac{s(l,m+1)-s(l,m-1)}{s(l+1,m)-s(l-1,m)}\right) \quad (6)$$

Then the key point descriptor of size 128 element vector is obtained with help of histogram created around each location. Key point descriptor is calculated for all pair of band of images [8].

Further steps are as follows.

Let A_i and A_j be two hyperspectral band images.

i) Evaluate key point descriptor for the two band images A_i and A_j.

ii) Find the matching scores for all keypoints in the band images. A matching is valid if the feature vector distance is below the threshold distance ratio.

iii) Using the matching score and keypoints, the dissimalirity matrix (D_{ij}) between any two bands in hyperspectral image is given by

$$Dij = 100[1 - (\frac{Mij}{\min(ki,kj)}] \quad (7)$$

Where

i,j denotes band images in hyperspectral data

K_i denotes the number of key points in hyperspectral images

M_{ij} denotes the maximum number of key point matches.

The dissimilarity matrix obtained for Jasper Ridge hyperspectral image is as depicted in Fig.5.

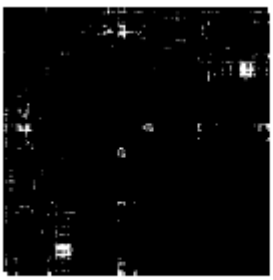


Fig.5: Dissimilarity Matrix-Jasper Ridge image

Let e X f be the dimension of dissimilarity matrix where e and f represents the band number in the original image. For example, in the Jasper Ridge image we have 198 bands therefore the dissimilarity matrix size is of 198X198.The first row represents band 1 dissimilarity value with the remaining bands. Diagonal value of the matrix is zero since it represent the matching between the same bands, for example band1-band1, band2-band2,..etc [10].The computational operations is not increased since SIFT is done only once and matching performed twice for the band images. Further, this matching score helps to differentiate two materials with more or less same spectral signatures during extraction of end members [2].

5. End Member Extraction

End members are the pure spectral signature for a single material substance. End member is not a pixel; it represents the reflected values over the spectral range used to capture the image[14]. There are two ways of identifying end members in hyperspectral images namely End member Extraction algorithm (EEA) and End Member Generation Algorithm (EGA).EEA is a direct method of extracting pure materials from the input whereas EGA is a method of extracting pure signatures from the given ground truth pure materials[15]. To highlight the proposed dimension reduction technique N -FINDR method is used for spectral unmixing application in hyperspectral images [22].

5.1. N-FINDR

This end member extraction algorithm is an unsupervised technique to find the different materials in linear mixtures of pure end member spectra. The basic concept behind this algorithm is randomly choosing the location and updating it based on volume calculation [16].

N FINDR works by growing a simplex inside the data, beginning with a random set of pixels as initial end members.

Step 1: Let 'p' no.of end members be

$$\left\{m_1^{(0)}, m_2^{(0)}, \ldots m_p^{(0)}\right\} \quad (7)$$

$$vo\left\{m_1^{(k)}, m_2^{(k)}, \ldots m_p^{(k)}\right\} = \frac{\det(m_1^{(1)}, m_2^{(1)}, \ldots m_p^{(1)})}{(p-1)!} \quad (8)$$

Step 2: Volume calculation,

S**tep 3:** Volume recalculation for the sample vector 's',

$$vo\left\{s, m_2^{(k)}, \ldots m_p^{(k)}\right\}, vo\left\{m_1^{(k)}, s, \ldots m_p^{(k)}\right\} \ldots vo\left\{m_1^{(k)}, m_2^{(k)} \ldots s\right\} \quad (9)$$

If the volume calculated for sample's' is greater than the volume calculated in step2, then that vector is selected as the final end members. The same process is repeated until all spectral signatures are obtained.

5.2. Abundance Map Generation

Fully Constrained least square estimation (FCLS) is used to generate abundance maps for the spectral signature extracted from N-FINDR algorithm [16].

Each pixel in hyperspectral image consists of linear combination of 'p' end members and added noise modeled as

$$X \approx E_\alpha + n = \sum_{i=1}^{p} \rho_i \alpha_i + n \quad (10)$$

Where

$E = \{m_i\}_{i=1}^{p}$ is the end member

$\alpha = \{\alpha_1, \alpha_2 \ldots \alpha_p\}$ is 'p' dimensional vector

n is noise

Two constraints on the abundance co-efficient are positivity and sum to one, expressed mathematically as

$$\sum_{i=1}^{p} \alpha_i = 1, \max_{\alpha \in \Delta}\{(X - \alpha E)^T (X - \alpha E)\} \quad (11)$$

And

$$\sum_{i=1}^{p} \alpha_i = 1, \min_{\alpha \in \Delta}\{(X - \alpha E)^T (X - \alpha E)\} \quad (12)$$

Unconstrained solution is

$$\alpha \approx (E^T E)^{-1} E^T X \quad (13)$$

where α is the minimum reconstructed abundance map error obtained resulting in an output similar to ground truth.

6. Proposed Work

Hyperspectral cube with high dimension is an input to the proposed system and all bands affected by water vapor, atmospheric effects are removed for further data analysis. This is a common procedure to be used before processing any hyperspectral data. The next step is the dimension reduction technique to have only few informative bands from large number of hyperspectral band and which is the necessary pre-processing technique to be used to reduce the computational complexity. Our proposed SIFT based band selection pre-processing dimension reduction method reduces 224 bands in original hyperspectral image to 'p' informative bands. Further, end member extraction N FINDR and FCLS algorithm is used to determine abundance maps [8].The proposed methodology is depicted as a diagram in Fig. 6.

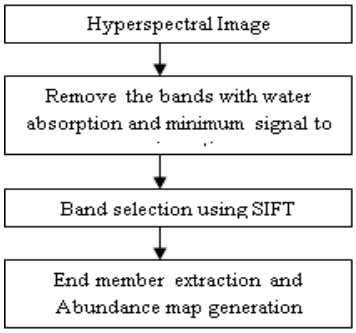


Fig.6: Proposed work flow diagram

The implementation steps of the algorithm are as follows.

1. Remove the low SNR bands and water absorption bands.
2. The scale invariant features (SIFT) are calculated for each band in an image.
3. Then the dissimilarity matrix is obtained from SIFT feature matching points between all the bands in an image.
4. The informative bands are selected from dissimilarity matrix by fixing the threshold't'.
5. Using N FINDR, end members are extracted and abundance maps are generated using fully constrained least square estimation.

7. Implementation Results

Jasper Ridge, an AVIRIS hyperspectral data of size 100X100 pixels with 224 bands is used for implementation. Removing the low SNR and water absorption bands, 108 bands are preserved for further processing. In our experimentation, preserving maximum information the original number of bands for further applications in unmixing, classification are reduced from 224 to 'p' bands using SIFT based dimension reduction technique. The proposed dimension reduction technique is used as a pre-processing for spectral unmixing application. Spectral unmixing used to obtain the end members and their abundance maps. The abundance maps generated are compared with ground truth abundance maps using abundance angle distance (AAD) and average AAD as a performance measure [6]. To justify the proposed technique, two other existing methods namely PCA based Unmixing and LDA based unmixing are taken as comparison methods [17]. The results are tabulated in Table.1-3.AAD value is the performance measure for estimating abundances of end members. AAD is calculated using the formula

$$AAD = \cos^{-1}\frac{(a_g . a_i^t)}{(\|a_g\| . \|a_i^t\|)} \quad (14)$$

Where a_g represents ground truth abundance vector and a_i^t represents transpose of extracted abundance vector.

From the AAD value, it is clear that our proposed dimension reduction technique performs well compared to the existing methods. The N- FINDR algorithm extracts the end members and their abundance maps are estimated using fully constrained least square method. Abundance maps are estimated for each and every end member extracted from N- FINDR .The ground truth abundance maps are available which is used to find the AAD value. The proposed algorithm is also experimented on SAMSON image of size 95 X 95 with 156 bands. The abundance map results were discussed here only for Jasper Ridge image.

Average Abundance angle distance (A- AAD) is used to analyze the overall performance of abundance maps.

$$A - AAD = \sqrt{\frac{1}{p}\sum_{i=1}^{p}(AAD)_i^2} \quad (15)$$

where $(AAD)_i$ is the AAD value for 'p' end members.

The minimum A- AAD value, abundance map obtained is similar to ground truth abundance map. The abundance maps for the ground truth image and proposed technique are as shown in Fig.7 and Fig.8.

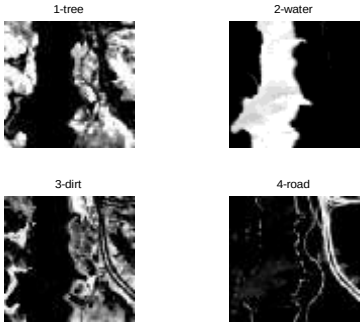


Fig.7: Ground Truth Abundance Maps

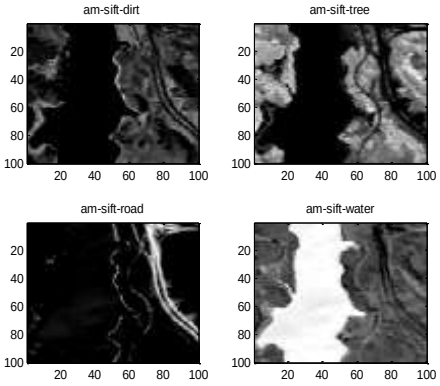


Fig.8: Abundance Maps – Proposed Method

The abundance maps of PCA and LDA based unmixing techniques are as shown in Fig.9 and Fig.10.

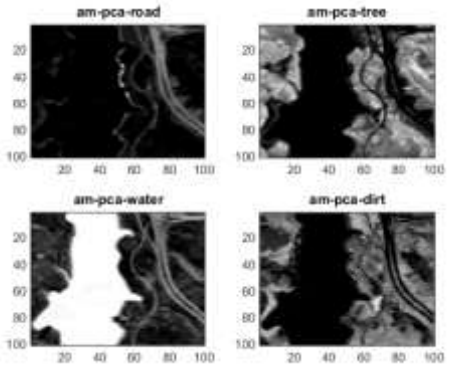


Fig.9: Abundance Maps-PCA method

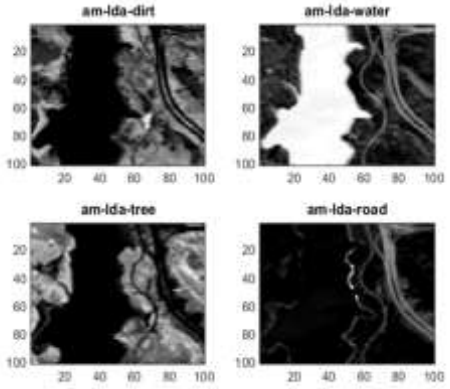


Fig.10: Abundance Maps-LDA method

The following Table.1 and Table.2 displays the Abundance Angle Distance (AAD) value of the methods implemented for two set of real image.

Table 1: Jasper-ridge – AAD

End members	PCA	LDA	SIFT
Tree	0.1618	0.1617	0.1554
Road	0.1219	0.1151	0.0921
Water	0.2087	0.1999	0.2673
Dirt	0.1298	0.1236	0.2044

Table 2:. Samson – AAD

End members	PCA	LDA	SIFT
Rock	0.2611	0.2490	0.1826
Tree	0.2596	0.1976	0.2652
Water	0.4299	0.3829	0.3802

The average –AAD used as the overall performance measure analysis is depicted in table 3.

Table 3: Average - AAD

Jasper -Ridge		Samson	
Methods	Average – AAD	**Methods**	Average – AAD
PCA	0.1591	**PCA**	0.3267
LDA	0.1536	**LDA**	0.2972
SIFT	0.1403	**SIFT**	0.2875

From the above simulation results, it is clear that our proposed dimension reduction technique performs well compared to the existing methods. The abundance map shown in Figure 8, particularly the water map extraction is better in the proposed method compared to two other existing techniques. The abundance map performance parameters are depicted as a bar chart in Fig.11-13.

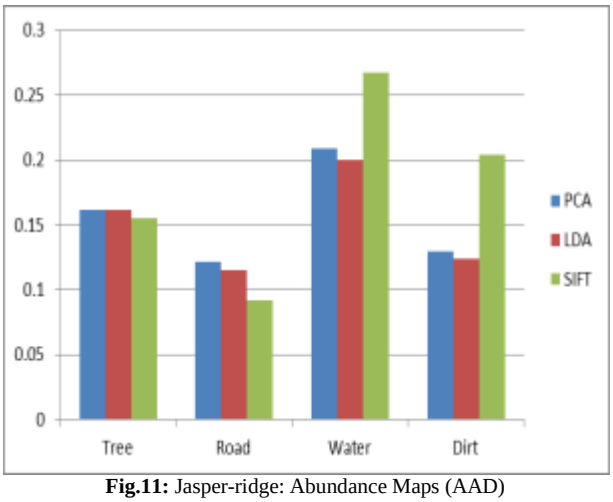


Fig.11: Jasper-ridge: Abundance Maps (AAD)

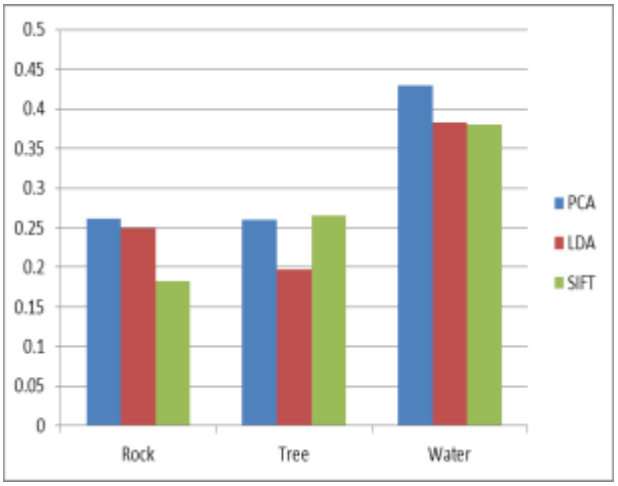


Fig.12: Samson: Abundance Maps (AAD)

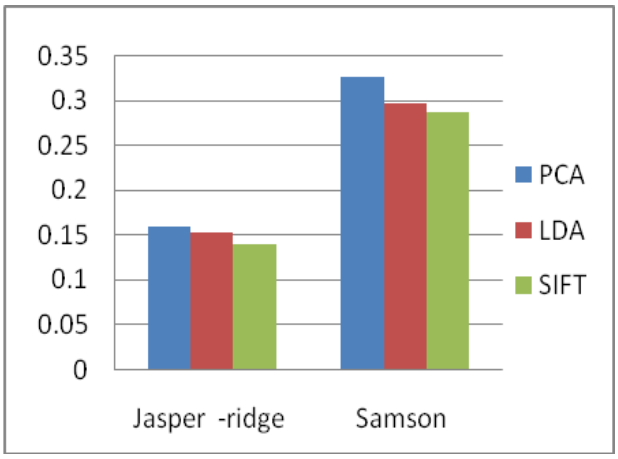


Fig.13: Average AAD (A-AAD)

8. Conclusion

The proposed method of SIFT dimension reduction followed by application in unmixing performs better compared to existing PCA and Discriminant analysis based unmixing. The main advantage of SIFT is its scale invariance to blur, rotation and illumination. The experimental results also show that abundance maps extracted with reduced bands are similar to ground truth maps resulting in a minimum AAD value. From the implementation results, the proposed band selection using SIFT is the promising and authentic dimension reduction technique. The proposed dimension reduction technique can be used as a pre-processing method for unmixing, classification and detection. Future work

involves determining initially the abundance percentage of each end member and then appropriately applying the unmixing technique to get accurate unmixing results.

References

[1] Antonio Plaza, Chein-I Chang(2005),An improved N-FINDR Algorithm in implementation Algorithms and Technologies for Multispectral, Hyperspectral, and Ultraspectral Imagery XI, Proceedings of SPIE,162-171.

[2] Alina Zare and K. C. Ho (2014), "Endmember variability in hyperspectral analysis: addressing spectral variability during spectral unmixing", IEEE Signal Processing Magazine 31, pp. 95-104.

[3] Alp Ertürk and Antonio Plaza (2015), "Informative change detection by unmixing for hyperspectral images", IEEE Geoscience and Remote Sensing Letters 12(6), pp.1252-1256.

[4] Barberis, G. Danese, F. Leoporati, A. Plaza and E. Torti (2013), "Real-time implementation of the vertex component analysis algorithm on GPUs", IEEE Geoscience and Remote Sensing Letters 10(2), pp. 251-255.

[5] Chang-Ci,Wu ,Tsai CT (2011),Random N-finder end member extraction algorithms for hyperspectral imagery,IEEE transcations on image processing,Vol .20(3), pp.641-656.

[6] D. G. Lowe (2004),"Distinctive image features from scaleinvariant keypoints," International Journal of Computer Vision, vol. 60(2), pp. 91-110.

[7] Inmaculada Dópido, Jun Li, Paolo Gamba and Antonio Plaza (2014), A New Hybrid Strategy Combining Semisupervised Classification and Unmixing of Hyperspectral Data, IEEE Journal of Selected Topics In Applied Earth Observations and Remote Sensing, VOL. 7, No. 8.

[8] John P. Ferguson (1981), "An Introduction to Hyperspectral Imaging", Photonics and Analytic Marketing Ltd,pp 100-110.

[9] J. M. P. Nascimento and J. M. Bioucas-Dias (2005), "Vertex component analysis: a fast algorithm to unmix hyperspectral data", IEEE Trans. Geosci. and Remote Sensing 43(4),pp. 898-910.

[10] J. M. Bioucas-Dias, A. Plaza, N. Dobigeon, M. Parente, Q. Du, P. Gader and J. Chanussot (2012), "Hyperspectral unmixing overview: Geometrical, statistical, and sparse regression-based approaches", IEEE J. Sel. Topics Appl. Earth Observations Remote Sensing 5(2),pp. 354-379.

[11] Jie Chen, Cedric Richard and Paul Honeine (2012), "Nonlinear unmixing of hyperspectral data based on a linear-mixture/nonlinear-fluctuation model", IEEE Trans. Signal Process. 1, pp. 480-492.

[12] Lei Yan, Sui-Hua Liu, Hui-Li-Liu, Xin Jing and Chengqi Cheng (2014), Two inverse processes: spectral reconstruction and pixel unmixing, 2014 Third International Workshop on Earth Observation and Remote Sensing Applications,pp.456-501

[13] Lodha,S.P.Kamapur(2014),"Dimension reduction for hyperspectral images",International Journal of innovation in engineering and management,IJAIEM,3(10).pp. 45-53.

[14] M. A. Veganzones, Guillaume Tochon, Mauro Dalla-Mura and A. J. Plaza (2014), Hyperspectral image segmentation using a new spectral unmixing based binary partition tree representation, IEEE Trans. Image Process. 23(8), pp.3574-3589.

[15] M.R.Vimala Devi,Dr.S.Kalaivani (2016),"A view on spectral unmixing in hyperspectral images",Far East Journal of Electronics and Communication, ,pp.23-32.

[16] N. Keshava and J. F. Mustard (2002), "Spectral unmixing", IEEE Signal Processing Magazine 19, pp.44-57.

[17] Nirmal Keshava (2003), "A survey of spectral unmixing algorithms", Lincoln Laboratory Journal 14(1), pp.55-78.

[18] Peg Shippert (1980), "Introduction to Hyperspectral Image Analysis", Earth Science Applications Research Systems.

[19] Panagiotis Antonapolus,Nikos Nikolaidis,Ionninis pitas (2009),"Hierarchical face clustering using SIFT fetures",IEEE International Conference on Mechtronics and Automation,pp. 234-240.

[20] Sergio Bernabe, Gabriel Martín,Guillermo Botella (2017),Parallel Implementation of a Full Hyperspectral Unmixing Chain Using OpenCL, IEEE Journal of Selected Topics in Applied Earth Observations and Remote Sensing ,10(6).

[21] W. Hapke (1981),Bidirectional reflectance spectroscopy",J. Geophys. Res. 86, pp. 3039-3054.

[22] W. Bao, Q. Li, L. Xin and K. Qu (2016), Hyperspectral unmixing algorithm based on Nonnegative Matrix Factorization,2016 IEEE International Geoscience and Remote Sensing Symposium (IGARSS), Beijing, ,pp. 6982-6985.doi: 10.1109/IGARSS.2016.7730821.